Thermal Chemistry of Styrene on Si(100)2×1 and Modified Surfaces: Electron-Mediated Condensation Oligomerization and Posthydrogenation Reactions

Q. Li and K. T. Leung*

Department of Chemistry, University of Waterloo, Waterloo, Ontario N2L 3G1, Canada

Received: August 25, 2004; In Final Form: November 5, 2004

The room-temperature (RT) adsorption and surface reactions of styrene on Si(100)2×1 have been investigated by thermal desorption spectrometry, low-energy electron diffraction, and Auger electron spectroscopy. Styrene is found to adsorb on Si(100)2×1 at a saturation coverage of 0.5 monolayer, which appears to have little effect on the 2×1 reconstructed surface. The chemisorption of styrene on the 2×1 surface primarily involves bonding through the vinyl group, with less than 15% of the surface moiety involved in bonding through the phenyl group. Except for the 2×1 surface where molecular desorption is also observed, the adsorbed styrene is found to undergo, upon annealing on the 2×1, sputtered and oxidized Si(100) surfaces, different thermally induced processes, including hydrogen abstraction, fragmentation, and/or condensation oligomerization. Condensation oligomerization of styrene has also been observed on Si(100)2×1 upon irradiation by low-energy electrons. In addition, large postexposure of atomic hydrogen to the chemisorbed styrene leads to Si−C bond cleavage and the formation of phenylethyl adspecies. Hydrogen therefore plays a decisive role in stabilizing and manipulating the processes of different surface reactions by facilitating different surface structures of Si.

1. Introduction

For several decades, the rapid pace of progress in the semiconductor industry has been demonstrated with the most frequently cited trend in "integration level". The so-called Moore's law (the number of components per chip doubles every 18 months)[1] has become a perpetual challenge to modern technologies in developing new solutions for the miniaturization of electronic devices, which is rapidly approaching the nanometer scale.[2] Due to their unique physical and electronic properties, organic semiconductors represent a viable material for improving both the functionality and miniaturization,[3] and they promise new technological applications in the emerging nanoelectronics industry.[4−7] Many applications of organic semiconductors rely on the synthesis of fully conjugated organic polymers, or conducting polymers.[8] Molecular engineering of π-conjugated oligomers and polymers has therefore become especially important to producing well-characterized organic nanoscale structures and devices.[9]

Si(100) is one of the most important substrates for fabrication of microelectronic devices.[10,11] With its special structural and electronic properties,[12,13] particularly the close analogy of Si dimers to a carbon−carbon double bond (C═C), Si(100) provides an ideal platform for building hybrid devices by seeding unsaturated hydrocarbons on the template generated by the directional dangling bonds of the (100) surface. Recent studies of the interactions of unsaturated hydrocarbons with Si(100) have exploited many promising opportunities for the development of atomically well-defined and ordered surface functionalities that form the basis of molecular devices and nanoelectronics as well as biotechnology.[3,14,15]

Aromatic hydrocarbons (e.g., benzene) and chainlike alkenes (e.g., ethylene) are the basic building blocks for constructing "conjugated" structures in most conducting polymer materials.[8,9] Styrene (or vinylbenzene) therefore represents one of the most fundamental combinations of a hexacyclic aromatic unit (the phenyl group) with the smallest alkene (the vinyl group). The interaction of benzene with silicon has been the subject of extensive experimental[16−21] and theoretical studies.[22−27] These studies show that chemisorption of this homocyclic aromatic compound on Si(100)2×1 follows the Diels−Alder cycloaddition mechanism, giving rise to a di-σ-bonded cyclohexa-2,5-dien-1,4-diyl (and cyclohexa-3,5-dien-1,2-diyl) adsorption species. Adsorption of ethylene on Si(100) has also been well studied, both experimentally[28−33] and theoretically,[34−36] and is found to form a di-σ-bonded ethane-1,2-diyl with a Si dimer. Styrene is a particularly interesting molecule because, unlike benzene, the presence of a vinyl group in styrene provides the prospect of polymerization. Adsorption of styrene on Si(100) could therefore provide a benchmark system for investigation of surface interactions and processes that are prototypical of organic semiconductors.[3] Relative to benzene and ethylene, styrene is expected to undergo more complex yet selective chemisorption on Si(100). To date, only a limited number of studies have been made for styrene on Si(100) surfaces and none on the respective thermally or electron induced surface processes. In particular, a recent Fourier transform infrared (FTIR) spectroscopic study by Schwartz et al.[37] has shown that this high selectivity involves bonding through the vinyl group with the aromatic ring (the phenyl group) unperturbed. Using the tip of a scanning tunneling microscope (STM) to initiate adsorption of styrene on a H-terminated Si(100)2×1 surface, Lopinski et al.[38] have demonstrated self-directed growth of molecular wires along the direction of the Si-dimer row.

In the present work, we examine the interactions of styrene with the 2×1 and modified surfaces of Si(100) using thermal desorption spectrometry (TDS), low-energy electron diffraction (LEED), and Auger electron spectroscopy (AES) to better understand not only the important roles of the vinyl and phenyl groups in organosilicon surface chemistry but also the nature of different thermal surface processes for different surface

* Electronic mailing address: tong@uwaterloo.ca.

10.1021/jp0461605 CCC: $30.25 © 2005 American Chemical Society
Published on Web 01/05/2005

conditions. Factors that could be used to monitor and control plausible synthesis steps of well-defined organic semiconductors in the nanoscale are of particular interest. The present result is also compared with our earlier work on homocyclic (benzene and toluene)[39] and heterocyclic (pyridine) unsaturated hydrocarbons on Si(100).[40] In addition to the multitude of thermally induced processes (other than molecular desorption), the effects of low-energy electron irradiation and postexposure of atomic hydrogen to the adsorbed styrene are also investigated.

2. Experimental Section

The experimental setup and procedure for the TDS experiments have been described in detail elsewhere.[39] Briefly, the experiments were conducted in a home-built dual-chamber ultrahigh vacuum (UHV) system with a base pressure better than 5×10^{-11} Torr. A 12.5×3.5 mm^2 substrate was cut from a polished p-type B-doped Si(100) wafer (0.4 mm thick) with a resistivity of 0.0080−0.0095 Ω·cm. The Si sample was mechanically fastened to the sample holder at both ends by Mo supporting plates and retaining bars, with small Si spacers sandwiched between the Mo supports and the Si sample to minimize thermal contact between the sample and the rest of the manipulator while a good electrical connection was maintained. A type-K thermocouple, wrapped in a piece of Ta foil, was inserted between the Si spacers and mechanically fastened to one end of the Si sample by a Mo bar. A home-built programmable proportional−integral−differential temperature controller was used to provide linear temperature ramping at an adjustable heating rate, typically set at 2 K/s for the present TDS experiments.

Before introduction into the UHV chamber, the Si sample was precleaned by using a typical RCA procedure[41] that involves soaking in a basic peroxide solution consisting of equal parts of H_2O_2 (30%) and NH_4OH (30%) in 5−20 parts of water. This treatment was effective in both removing light organic contamination and providing a thin oxide film, which made the surface less susceptible to organic and particulate contamination.[42] After the bake-out, the sample was outgassed at 900 K for 20 h until the pressure recovered to below 2×10^{-10} Torr. The temperature of the sample was then rapidly increased to 1500 K while the vacuum was carefully kept below 1×10^{-9} Torr. Unlike benzene, styrene was found to be much more "sticky" on the Si surface, and any amount of carbon left after each anneal would cause a contamination problem if the surface was treated immediately with a high-temperature flash-anneal (a procedure commonly employed in STM experiments). Instead, the Si sample was first treated with several cycles of sputtering and low-temperature anneal (below 850 K), before a flash-anneal to 1500 K was applied. The cleanliness of the Si(100) surface was verified by AES with the near-surface carbon concentration below its detection limit (typically 5% for a retarding-field LEED optics) and by a sharp 2×1 LEED pattern at room temperature (RT). This cleaning method can be used to prolong the use of a single sample, and a Si sample could easily survive 50 TDS runs before replacement.

The chemicals [styrene (99+% purity), styrene-d_8 (98+% D purity), and styrene-*ring*-d_5 (98% D purity)] used in the present study were obtained commercially from Aldrich and Cambridge Isotope Laboratories and were degassed by repeated freeze−pump−thaw cycles prior to use. Sample dosing was performed by back-filling the sample preparation chamber with a precision leak valve to an appropriate pressure, as monitored by an uncalibrated ionization gauge. All exposures [in units of Langmuir (1 Langmuir $= 10^{-6}$ Torr·s)] were performed at RT unless stated otherwise.

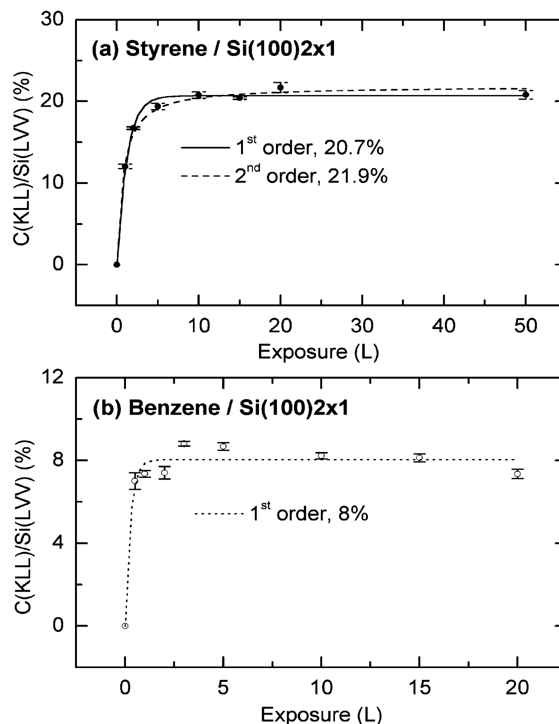

Figure 1. Relative carbon moiety as indicated by the peak-to-peak intensity ratio for the C(KLL) to Si(LVV) Auger transitions as a function of room-temperature exposure of (a) styrene and (b) benzene to Si(100)2×1. The experimental data are compared with fitted curves based on the first- and second-order adsorption kinetic equations.

3. Results and Discussion

3.1. RT Adsorption at Various Exposures. The adsorption of styrene on Si(100)2×1 at RT was studied as a function of exposure by LEED and AES. Upon different exposures of styrene to the Si(100) surface at RT, only a slight increase in the background intensity was observed in the two-domain (2×1) LEED pattern characteristic of a clean Si(100) surface, which shows that the dimer-row structure of the Si substrate is generally preserved after the adsorption of styrene. The peak-to-peak ratio of the C(KLL) Auger peak to that of the Si(LVV) Auger peak is used to indicate the relative carbon moiety. Figure 1 compares this ratio as a function of RT exposure for styrene and benzene on Si(100)2×1 and each with the corresponding results expected from first-order and second-order adsorption kinetics. Evidently, both the first- and second-order kinetics are in good accord with the experimental data, indicating that our present data may not be sufficiently sensitive to differentiate the adsorption order. For styrene, the ratio appears to reach its saturation value at 10 Langmuir exposure, which generally marks the completion of adsorption of the first monolayer (ML). The saturation coverage of benzene has been estimated to be 0.27 ML by Taguchi et al.[16] From the ratio of the saturation values of styrene (21.3%) and benzene (8.0%) and after the number of carbon atoms in styrene (8) and benzene (6) is taken into account, we determine the saturation coverage for styrene to be 0.5 ML, which corresponds approximately to one styrene molecule per Si dimer on the 2×1 surface.

Figure 2 shows the TDS profiles of mass 112 (parent mass) and mass 4 corresponding to molecular and recombinative D_2 desorption, respectively, for different RT exposures of styrene-d_8 on Si(100)2×1. It should be noted that deuterated styrene was used in our TDS experiments in order to avoid the large H_2 background commonly found in stainless steel UHV chambers. In addition to the parent mass (mass 112), other

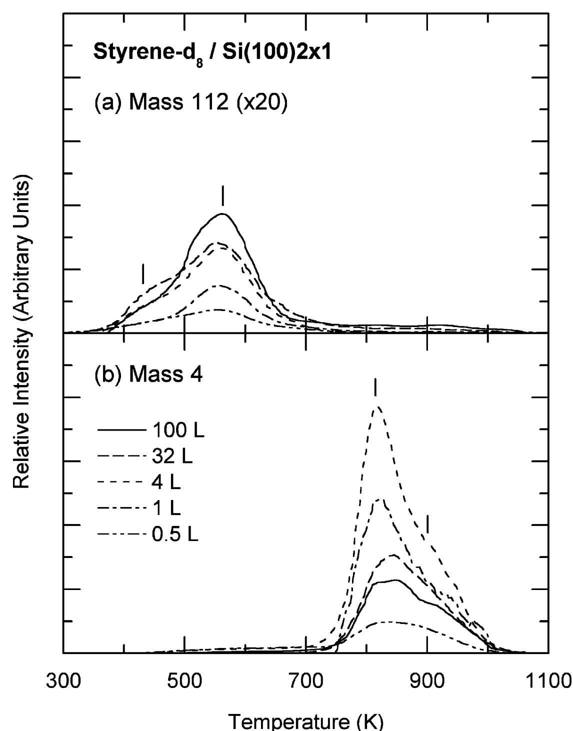

Figure 2. Thermal desorption profiles of mass 112 (parent mass) and mass 4 (D_2) as a function of room-temperature exposure of styrene-d_8 to Si(100)2×1.

smaller ionic fragments including mass 110 (C_8D_7), mass 84 (C_6D_6), and mass 56 (C_4D_4) were also monitored during the TDS experiments (not shown). Since their corresponding peak intensity ratios were found to be in good accord with the respective ratios in the cracking pattern of styrene-d_8[43] over the same temperature range (of 350−700 K) as that for mass 112, these smaller mass fragments could be attributed to dissociation of molecularly desorbed styrene-d_8 in the ionizer of the quadrupole mass spectrometer (QMS). These TDS profiles therefore indicate that styrene-d_8 desorbs molecularly from Si(100)2×1 over this temperature range. The TDS intensity for molecular desorption reaches saturation at ∼10 Langmuir exposure (not shown), which is in good accord with the AES result for the adsorption of styrene (Figure 1). Evidently, two desorption states are observed for molecular desorption (Figure 2). The primary feature for the molecular desorption of styrene is found to have a desorption maximum at 560 K. The similarity in the temperature of this desorption maximum to that for ethylene (590 K) on Si(100)2×1[28,29] suggests that the predominant chemisorption configuration involves di-σ bonding between the vinyl group and the Si dimer. This bonding geometry for styrene on Si(100)2×1 has also been concluded from an earlier FTIR study by Schwartz et al.[37] Moreover, a minor desorption pathway is found to exhibit a desorption maximum at 430 K, which is similar to those of the primary molecular desorption features found in our previous TDS studies on benzene, toluene,[39] and pyridine on Si(100)2×1.[40] This similarity suggests a similar molecular adsorption state involving bonding of the phenyl group, which may include di-σ-bonding to a single Si dimer[24] and/or tetra-σ-bonding to two Si dimers.[25] The relative intensity ratio of the two molecular desorption features at saturation coverage in Figure 2a shows that only 15% of desorption comes from phenyl-bonded structures (at 430 K) while the majority originates from vinyl-bonded structures (at 560 K). However, the phenyl-bonded structure has not been reported in the earlier FTIR work,[37] which could be due to the sensitivity of the FTIR technique in detecting weakly adsorbed species. Furthermore, the TDS feature for the phenyl-bonded adspecies (at 430 K) appears to reach saturation at a lower exposure than the feature for the vinyl-bonded adspecies (at 560 K), which is consistent with the larger footprint required for the phenyl-bonded structure.

To understand the geometries and binding energies for different adsorption structures, we performed ab initio density functional calculations for styrene interacting with a triple dimer $Si_{21}H_{20}$, employed for modeling the Si(100)2×1 surface, using the Gaussian 98 program.[44] In particular, the hybrid functionals consisting of Becke's three-parameter nonlocal exchange functional and the correlation functional of Lee−Yang−Parr (B3LYP)[45] were used along with the 6-31G(d) basis set. Figure 3 shows the optimized geometries for the vinyl-bonded (*cis*-phenylethene-1,2-diyl) and phenyl-bonded (2-vinylcyclohexa-2,5-diene-1,4-diyl) adsorption structures. The corresponding binding energies with zero-point energy corrections, ΔE, are found to be −35.2 and −23.4 kcal/mol, respectively, which is consistent with our assignment that the phenyl-bonded adspecies would be desorbed at a lower temperature than the vinyl-bonded adspecies (Figure 2a). Furthermore, similar calculations have been performed for ethylene and for benzene and found to have corresponding binding energies of −41.2 and −16.7 kcal/mol, respectively. The similar magnitudes of the calculated binding energies for the vinyl-bonded styrene and ethylene and those for the phenyl-bonded styrene and benzene further support our assignments for the molecular desorption features in Figure 2. It should be noted that improved calculations involving a larger basis set are not expected to significantly change the qualitative nature of the adsorption configurations. Other conformers of the cyclohexadienediyl adspecies have also been considered and found to have a smaller magnitude for the binding energy.

3.2. Hydrogen Evolution. In addition to the molecular desorption profiles, Figure 2 also shows the mass 4 (D_2) TDS profiles with maxima at 810 K for RT exposures of styrene-d_8 on Si(100)2×1. It should be noted that the TDS profiles for normal and deuterated styrene are found to be identical in our TDS experiment, indicating that isotopic effect is not important for the adsorption process. The desorption maximum at 810 K appears to be quite stationary with increasing exposure in the D_2 TDS profile (Figure 2b), which suggests predominant first-order kinetics as a result of recombinative molecular desorption from Si monohydride.[46,47] The slightly higher temperature of the desorption maximum from that of monohydride desorption by 20 K[46,47] and the broad mass 4 profile extending to 1000 K (Figure 2b) are related to contributions from different sources of atomic hydrogen on the surface during the thermal desorption process. As observed in our previous TDS studies for toluene[39] and pyridine on Si(100),[40] hydrogen abstraction of styrene near or below its molecular desorption temperature could generate a comparable moiety of atomic hydrogen and other dissociated products, which could undergo further hydrogen abstraction mediated by the surface at a higher temperature than that of molecular desorption. This hypothesis is supported by earlier studies.[37,48,49] In particular, the FTIR study by Schwartz et al.[37] also reported a Si−H stretching feature indicative of C−H bond cleavage in the vinyl group of styrene upon adsorption at RT. Furthermore, similar TDS behavior for hydrogen desorption has also been obtained by Taylor et al.[48] for the adsorption and decomposition of acetylene on Si(100)2×1. Using high-resolution electron energy-loss spectroscopy, Huang et al.[49] later found that the dissociation of adsorbed acetylene occurs via C−H bond breakage

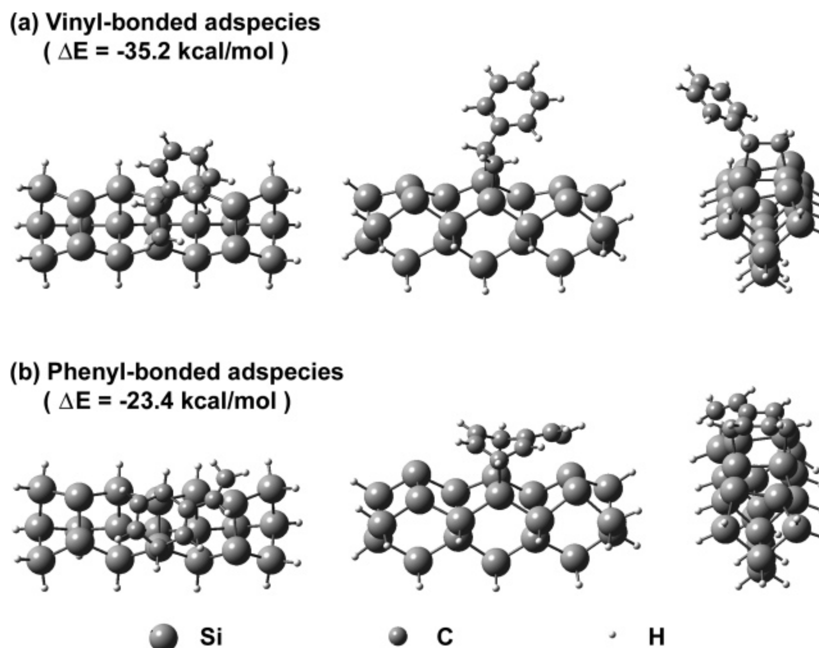

Figure 3. Schematic diagrams of the adsorption geometries in different perspectives and the corresponding adsorption energies ΔE obtained by a density functional calculation involving B3LYP/6-31G(d) for styrene on a model surface of $Si_{21}H_{20}$: (a) vinyl-bonded adspecies; (b) phenyl-bonded adspecies.

over a wide temperature range (>150 K) starting from 750 K, which is below the molecular desorption temperature of C_2H_2.

Similar to that observed for the adsorption of toluene on Si(100)2×1,[39] the intensity of D_2 desorption (Figure 2b) in the adsorption of styrene on Si(100)2×1 is over 10-fold higher than that for the corresponding molecular desorption (Figure 2a). However, unlike the molecular desorption that increases to a saturation level with exposure (10 Langmuir), the D_2 desorption reaches its maximum at ~4 Langmuir exposure of styrene-d_8 and then evidently decreases at a higher exposure (Figure 2b). This "anomalous" desorption behavior can be explained if the hydrogen abstraction is not instantaneous upon adsorption of styrene and it could be approximated as a separate step after the completion of the RT adsorption. As an example, we consider the simple case of complete hydrogen abstraction. Starting with an initial coverage of styrene θ (with its value between 0 and 1), which corresponds in effect to the occupancy per Si dimer, the change in the surface concentration of the adsorbed styrene, x, that undergoes hydrogen abstraction can be written as follows:

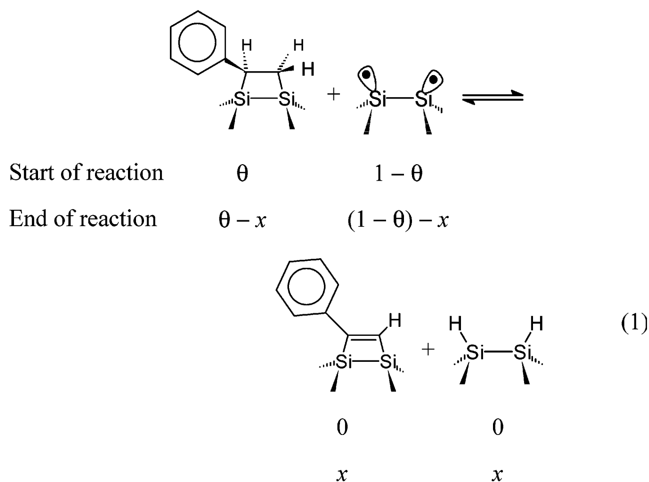

The maximum change x_{max} for complete hydrogen abstraction (reaction going to the right) would occur when $\theta - x \rightarrow 0$ or $(1 - \theta) - x \rightarrow 0$, that is, when $\theta = 0.5$ in this case. In our experiment, x_{max} is found to occur at a coverage of 0.8−0.9, which is larger than the value obtained for complete abstraction (0.5). This difference could be due to incomplete abstraction reaction at RT, as demonstrated by the amount of molecular desorption at a lower exposure (Figure 2a). Furthermore, the availability of vacated sites released in the thermal desorption process could also shift x_{max} to a larger exposure.

To determine whether the phenyl group is involved in the hydrogen abstraction of styrene, the TDS profiles for a 10 Langmuir RT exposure of styrene-*ring*-d_5 (i.e., with just the phenyl group deuterated) are compared with those of a similar exposure of styrene-d_8 to Si(100)2×1 in Figure 4. It should be noted that the TDS profile of mass 2 (H_2) for (normal) styrene has also been obtained (not shown) and found to be essentially identical to the corresponding TDS profile of mass 4 (D_2) for styrene-d_8 on Si(100)2×1 (Figure 4b), indicating that our present result is not sufficiently sensitive for detecting any weak kinetic isotope effect. Similarly to that shown in Figure 2 (Figure 4b), the molecular desorption depicted in Figure 4a is considerably weaker than the hydrogen evolution. The TDS profiles of the parent mass for styrene-*ring*-d_5 (mass 109) and styrene-d_8 (mass 112) are effectively identical. The integrated intensity and the overall shape of the sum of the mass 2 TDS profile (with desorption maximum at 800 K) and mass 4 TDS profile (with desorption maximum at 870 K) for styrene-*ring*-d_5 (Figure 4a) are found to be similar to those of the mass 4 TDS profile for styrene-d_8 (Figure 4b), which indicates that hydrogen abstraction can occur not just from the vinyl group but also from the phenyl group at a higher temperature. Below 700 K, the hydrogen atoms abstracted from the vinyl group of the adsorbed styrene evidently dominate the monohydride state on the Si(100)2×1 surface, and these hydrogen atoms start to desorb near 600 K. Above 700 K, on the other hand, the majority of hydrogen abstraction comes from the phenyl group. The present TDS results are consistent

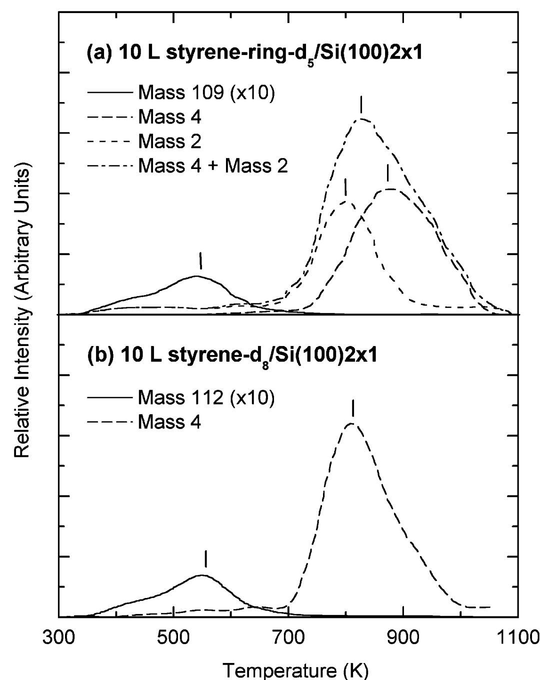

Figure 4. Thermal desorption profiles (a) of mass 109 (molecular desorption), mass 4 (D_2), and mass 2 (H_2) for a 10 L room-temperature exposure of styrene-*ring*-d_5 and (b) of mass 112 (molecular desorption) and mass 4 (D_2) for a 10 L room-temperature exposure of styrene-d_8, both to Si(100)2×1.

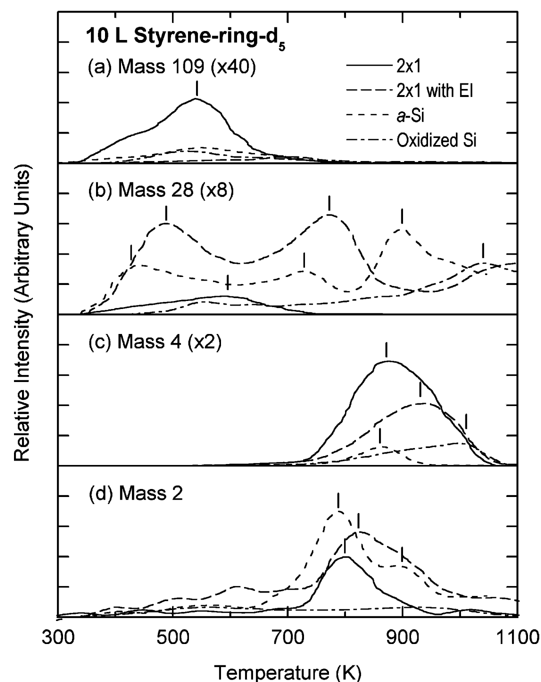

Figure 5. Thermal desorption profiles for (a) mass 109 (molecular desorption), (b) mass 28 (dissociative products), (c) mass 4 (D_2), and (d) mass 2 (H_2) for a 10 L room-temperature exposure of styrene-*ring*-d_5 to Si(100)2×1 without and with electron irradiation (EI) at 200 μA and 80 eV for 30 min, and to amorphous (*a*-) Si, and oxidized surface of Si(100).

with the FTIR study by Schwartz et al.[37] In particular, from the FTIR spectra recorded at RT for a 10 Langmuir RT exposure of styrene-d_3 (i.e., with just the vinyl group deuterated) to Si(100)2×1, Schwartz et al.[37] observed the emergence of the Si−H stretching mode (at 2060 cm^{-1}) upon annealing to 500−700 K (in addition to the Si−D stretch found at RT), which indicates that hydrogen evolution from the phenyl group occurs at the higher temperature. In the aforementioned di-σ vinyl-bonded geometry of styrene on Si(100)2×1 observed at RT, the "dangling" phenyl group is unattached to the Si surface, which gives rise to a similar FTIR spectrum as that of a free benzene molecule but different from that of benzene adsorbed on Si(100)2×1 in a cyclohexadiene-like adsorption geometry [as supported by the lack of C−H stretching vibration involving sp^3-hybridized (alkanelike) carbons].[37] Upon thermal excitation during annealing, the "dangling" phenyl group could become sufficiently close to the Si surface and attach to a substrate Si atom with the release of a phenyl H atom (onto a Si monohydride site) shown schematically below:

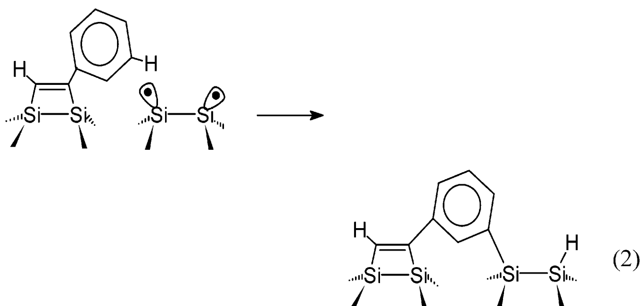

(2)

The attachment (bridging) of the phenyl group onto a second Si dimer is supported by the reduction in the number of FTIR features in the 3010−3080 cm^{-1} region,[37] indicative of the general increase in the number of hydrogen substitutions and replacements by bonding to the surface.[50] This picture is also consistent with a higher desorption maximum for recombinative desorption of the phenyl H atoms (870 K) than that of the vinyl H atoms (800 K). Another possible pathway for hydrogen evolution from the phenyl group is through adsorbate−adsorbate interaction, that is, condensation oligomerization, which will be discussed in more detail elsewhere.[51]

3.3. Electron Irradiation of Styrene on Si(100)2×1. Figure 5 shows the effects of low-energy electron irradiation on the TDS profiles of masses 109 (parent mass), 28, 4, and 2 for a 10 Langmuir RT exposure of styrene-*ring*-d_5 to Si(100)2×1. Electron irradiation (EI) was performed on the Si sample (held at 80 V bias potential) for 30 min at 0.2 mA with electrons thermionically emitted from a hot W filament positioned 5 cm away. Evidently, electron irradiation greatly diminishes desorption of the parent mass (Figure 5a), suggesting a significantly reduced moiety of molecularly adsorbed styrene on the electron-irradiated sample, which is likely due to electron-induced desorption[52] or to conversion to other (smaller dissociated or larger oligomerized) adspecies. In addition to the parent mass (mass 109), other smaller ionic fragments including mass 108 ($C_6D_5C_2H_2$), 83 (C_6D_5H), and 54 ($C_4D_2H_2$) were also monitored during the TDS experiments. The TDS profiles of these smaller fragments (not shown) closely follow that of the parent mass, indicating that they originate from dissociation of the molecularly desorbed styrene-*ring*-d_5 in the ionizer of the QMS. On the other hand, the TDS profile of mass 28 (Figure 5b) corresponds to desorption of dissociated fragments (C_2D_2 or C_2H_4) arising from electron irradiation of the adsorbed styrene. Without EI, only a very weak mass 28 desorption feature can be found in the 350−700 K region, generally indicating relatively weak dissociation of styrene (into smaller hydrocarbon fragments) upon adsorption and during the TDS experiment. Electron irradiation appears to significantly enhance the desorption profile of mass 28 (Figure 5b) with two desorption maxima at 480 and 760 K. Because the molecular desorption

maximum for C_2H_4 on Si(100)2×1 is normally found at 550 K,[29] the desorption maximum of mass 28 at 480 K can be attributed to the dissociative desorption resulting from the vinyl group of the styrene adsorbed on Si(100) upon EI. The lower temperature for the desorption maximum observed for the present case (480 K) than that for ethylene (550 K) is consistent with the less negative binding energy calculated for the vinyl-bonded styrene (−35.2 kcal/mol, Figure 3a) relative to that for C_2H_4 (−41.2 kcal/mol, see section 3.1). Furthermore, molecular desorption of acetylene from Si(100)2×1 has been reported with a desorption maximum at 690−740 K.[48] The desorption maximum for the higher-temperature feature of mass 28 (at 760 K) in Figure 5b could therefore be attributed to C_2D_2, which is evidently produced by electron-induced dissociation of the phenyl-d_5 group of the adsorbed styrene-*ring*-d_5 at RT.

The majority (~90%) of the mass 2 desorption for the electron-irradiated sample is found to occur above 700 K with a desorption maximum at ~800 K, which is similar to that found for styrene-*ring*-d_5/Si(100)2×1 without electron irradiation (Figure 5d). The small amount of desorption at 450−650 K could correspond to H_2 originated from the cracking of some dissociative products. On the other hand, there is a considerable reduction in the relative intensity and a discernible shift in the desorption maximum from 870 to 930 K for the mass 4 TDS profile for the adsorbed styrene-*ring*-d_5 upon electron irradiation (Figure 5c). The reduction in the relative intensity of the mass 4 TDS profile could be due to the reduced moiety of phenyl group caused by electron-induced dissociation to produce fragments such as C_2D_2 (mass 28). Hydrogen evolution could be due to recombinative desorption of H atoms abstracted from the adsorbates or to condensation oligomerization of the adsorbates. In the latter case, the reduced surface mobility and enhanced steric effect of larger molecules (oligomers) are expected to introduce a higher reaction activation barrier that requires a correspondingly higher temperature to overcome. Detailed mechanisms about hydrogen evolution in cyclic hydrocarbons on Si(100) are discussed elsewhere.[51] In particular, surface condensation oligomerization of pyridine on Si(100)2×1 at RT was found upon low-energy electron irradiation at RT.[40] In this case, the condensation oligomerization process was marked by a shift in the TDS maximum for hydrogen evolution to a higher temperature (910 K) relative to that of recombinative desorption from monohydrides abstracted from adsorbed pyridine monomers or its smaller fragments (~800 K). Together with the small shoulder appearing at 930 K of the mass 2 TDS profile (Figure 5d), the similarity in the observed shift in the desorption maximum for mass 4 in styrene-*ring*-d_5 (Figure 5c) suggests electron-induced oligomerization of styrene at RT, as in the case proposed for pyridine.[40] In accord with our previous TDS experiments,[51] the present work appears to support the general observation that the larger the size of the unsaturated organic adsorbate, the higher the temperature for hydrogen evolution. For instance, the desorption maximum for hydrogen evolution is found to increase from 790 K for surface monohydride to 800 K for vinyl group (Figure 4a), 870 K for phenyl group (Figure 4a), and 930 K for oligomers (Figure 5c) observed in the present work.

3.4. Surface Conditions Study. For completeness, we also compare in Figure 5 the TDS profiles for molecular desorption (mass 109) and desorption of dissociative products (masses 28, 4, and 2) for the 2×1 surface with those for the modified surfaces of Si(100) exposed to 10 Langmuir of styrene-*ring*-d_5 at RT. The amorphous Si (*a*-Si) surface was produced by ion sputtering in 4×10^{-5} Torr of Ar at 1 keV ion impact energy for 20 min, while the oxidized Si(100) surface was obtained by exposing a clean 2×1 surface with 100 L of O_2 at RT. The lack of any long-range order for both *a*-Si and oxidized Si surfaces was confirmed by the absence of a LEED pattern (below 100 eV electron beam energy).

The shapes and desorption maxima of the TDS profiles for molecular desorption (mass 109, Figure 5a), D_2 (mass 4, Figure 5c), and H_2 (mass 2, Figure 5d) for *a*-Si are found to be similar to those observed on the clean Si(100)2×1 surface. For *a*-Si, the TDS intensities for molecular and D_2 desorption are found to be greatly reduced (by over 70%), in contrast to an increase in the H_2 desorption, all relative to the 2×1 surface. The reduction in molecular desorption is likely due to the loss of Si dimer sites (appropriate for molecular adsorption) on the *a*-Si surface. In contrast to the generally weak and broad band of mass 28 for the 2×1 surface at 600 K, there are three strong mass 28 desorption features centered at 440, 730, and 900 K for *a*-Si (Figure 5b). On the other hand, the TDS profile of mass 26 (not shown) reveals a single desorption feature near 730 K for the *a*-Si sample. From the earlier work,[48] the mass 28 desorption feature at 730 K could only come from desorption of acetylene (C_2D_2), which should also exhibit a corresponding mass 26 (C_2D) TDS profile at approximately 20% of the TDS intensity of the parent mass (C_2D_2) according to the cracking pattern of acetylene.[43] After removal of this contribution due to C_2D_2 (with its origin likely coming from the dissociation of the phenyl group of the adsorbed styrene-*ring*-d_5) in the mass 26 TDS profile, we obtain a similar amount of contribution from the parent mass of C_2H_2 (as that originated from C_2D_2), which could come from dissociation of the vinyl group. Given the lack of any discernible features of mass 26 at the corresponding temperatures, the other TDS features of mass 28 at 440 and 900 K (Figure 5b) could be attributed to dissociative desorption of C_2D_2 from the phenyl group of adsorbed styrene-*ring*-d_5. The increase in the mass 28 TDS profile for *a*-Si surface with respect to that for the 2×1 surface (Figure 5b) suggests that there are evidently more active sites available for dissociation on the *a*-Si surface.

Figure 5 also shows the TDS profiles of masses 109, 28, 4, and 2 for a 10 Langmuir RT exposure of styrene-*ring*-d_5 on an oxidized Si(100) surface. Evidently, the total amounts of desorption of molecular (mass 109, Figure 5a) and dissociative products (mass 28, Figure 5b) are found to decrease significantly with respect to that for Si(100)2×1, while the corresponding TDS profile of mass 2 (Figure 5d) is reduced to featureless, which could be attributed to the loss of active adsorption sites due to oxidation. In particular, the lack of any discernible mass 2 (H_2) desorption suggests that hydrogen abstraction from the vinyl group on the 2×1 surface is blocked by the passivation of Si dangling bonds by oxygen. Passivation of the active sites can also be achieved by H atoms as demonstrated in a separate TDS experiment for styrene-d_8 on a H-terminated Si(100)1×1 surface, in which no desorption of mass 112 (parent mass of styrene-d_8), 28, or 4 was observed (not shown). On the other hand, the TDS intensity of mass 28 for the oxidized surface is found to increase considerably and shift toward a higher temperature with respect to that for the 2×1 surface (Figure 5b). The lack of any corresponding lower mass fragments, for example, mass 26, suggests that mass 28 is not due to desorption of C_2D_2 or C_2H_4 fragments but possibly to associative desorption of CO. Since the temperature of the desorption maximum for molecular desorption of CO on Si(100) (180 K)[53] [with the corresponding adsorption energy of CO on Si(100)2×1 estimated to be −(17−19) kcal/mol[54]] is found to be considerably

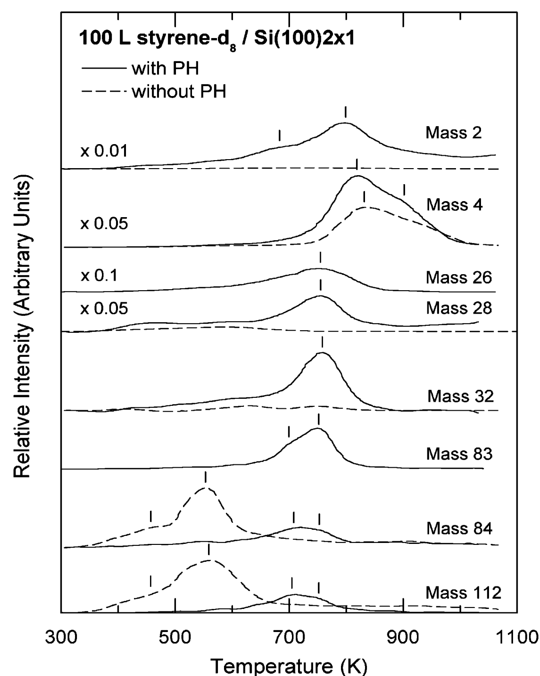

Figure 6. Comparison of thermal desorption profiles of mass 2, 4, 26, 28, 32, 83, 84, and 112 for a 100 L room-temperature exposure of styrene-d_8 to Si(100)2×1 surface, with and without posthydrogenation (PH).

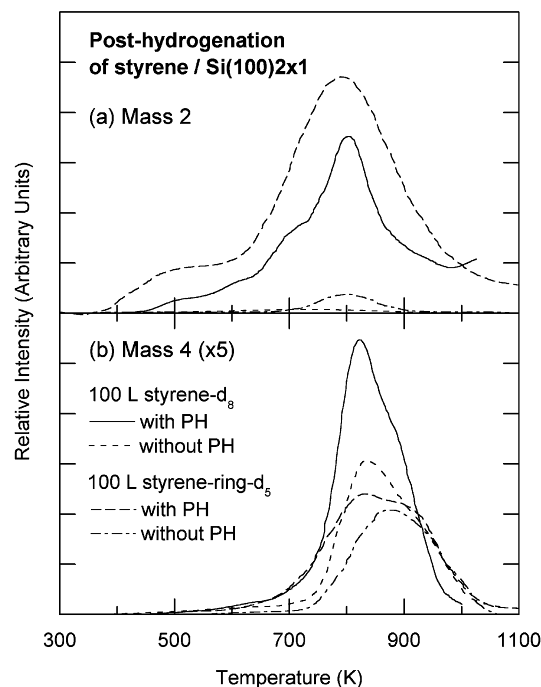

Figure 7. Comparison of thermal desorption profiles of (a) mass 2 and (b) mass 4 for a 100 L room-temperature exposure of styrene-d_8 with those of styrene-d_5 to Si(100)2×1, with and without posthydrogenation (PH).

lower than the observed desorption maximum (1040 K) in Figure 5b, other dissociation channels by which C readily combines with O on the oxidized surface to produce the desorbed CO could be activated (Figure 5b). The latter is consistent with an ascending shape and shift of the observed mass 4 TDS intensity toward the higher temperature side (Figure 5c) similar to the mass 28 profile (Figure 5b), which could be due to hydrogen evolution in this high-temperature region.

3.5. Surface-Mediated Hydrogenation Reactions. To investigate the interaction of atomic hydrogen with styrene adsorbed on Si(100)2×1, the sample saturated with a 100 Langmuir RT exposure of styrene-d_8 was postexposed with H atoms generated from 3000 L of H_2 with a hot W filament positioned 2 cm away. To minimize the effect of radiative heating from the hot filament during the hydrogen activation, liquid nitrogen was used to keep the sample near or below RT. After the posthydrogenation (PH), the diffused 2×1 LEED pattern for the styrene-d_8 saturated surface was changed to a 1×1 pattern, which indicates total destruction of the surface reconstruction involving the Si dimers. Evidently, the TDS features for the molecular (mass 112) desorption from both phenyl-bonded adspecies (at 460 K) and vinyl-bonded adspecies (at 560 K) shown in Figure 6 are greatly diminished. However, new desorption states with maxima at 700 and 750 K are observed for the posthydrogenated sample. The nature of these two states will be discussed below. Like the case without posthydrogenation, the mass 84 (C_6D_6) TDS profile for the sample with posthydrogenation appears to follow the TDS profile of the parent mass, which suggests that mass 84 is due to electron dissociation of the molecularly desorbed styrene-d_8 in the ionizer of the QMS. The stronger TDS maxima of mass 83 (C_6D_5H) and of masses 32 (C_2D_4), 28 (C_2D_2 or C_2H_4), and 26 (C_2H_2), all at 750 K, suggest that these fragments are predominantly due to associative desorption of H (from the surface) with the phenyl group and with the vinyl group, respectively, both of which involve isotopic mixing of H and D. Similar increase in the temperature of desorption maxima for molecular desorption has also been reported in our earlier studies on (methyl)cyclohexene and (methyl)cyclohexadiene on Si(111)7×7,[55-57] the TDS profiles of which provide strong evidence for the production of (toluene) benzene by dehydrogenation on Si(111)7×7 upon the TDS process. The desorption maxima for both molecular and dehydrogenated products were also found to be shifted by 100 K to 670 K, similar to the desorption maximum of dihydride (650 K). We have also performed the same TDS experiment for 100 Langmuir exposure of styrene-*ring*-d_5 with posthydrogenation. Results similar to those for styrene-d_8 have been observed for the corresponding masses: 109 (parent mass of $C_6D_5C_2H_3$), 83 (C_6D_5H), 30 ($C_2D_2H_2$), 28 (C_2D_2 or C_2H_4), and 26 (C_2H_2) (data not shown).

In Figure 6, the two intense TDS features of mass 2 with maxima at 680 and 800 K for the posthydrogenated styrene-d_8/Si(100)2×1 sample are found to be similar to those arising from recombinative thermal desorption, respectively, from dihydride and monohydride on a H-terminated Si(100) surface.[46,47] Two mass 4 TDS features with maxima located at 820 and 900 K are found for the posthydrogenated sample (Figure 6). In comparison with the TDS profile for the styrene-d_8/Si(100) sample without H postexposure, the corresponding mass 4 TDS profile for the posthydrogenated styrene-d_8/Si(100) sample nearly doubles in intensity, in marked contrast to that for the posthydrogenated styrene-*ring*-d_5/Si(100) sample, which is at about the same intensity as the styrene-d_8/Si(100) sample without H postexposure (Figure 7b). The increase in the D_2 desorption for the styrene-d_8/Si(100) sample with H postexposure can therefore be attributed to hydrogen abstraction from the vinyl group.

It is of interest to note that the TDS profile has not revealed any higher masses than the parent mass (e.g., mass 114), which would correspond to desorption of hydrogenated products of the adsorbed styrene. However, the TDS profiles of lower masses such as mass 84 (benzene-d_6) and 83 (benzene-d_5) follow that of mass 112 (parent mass of styrene-d_8), which suggests that hydrogenation occurs primarily for the vinyl group of the

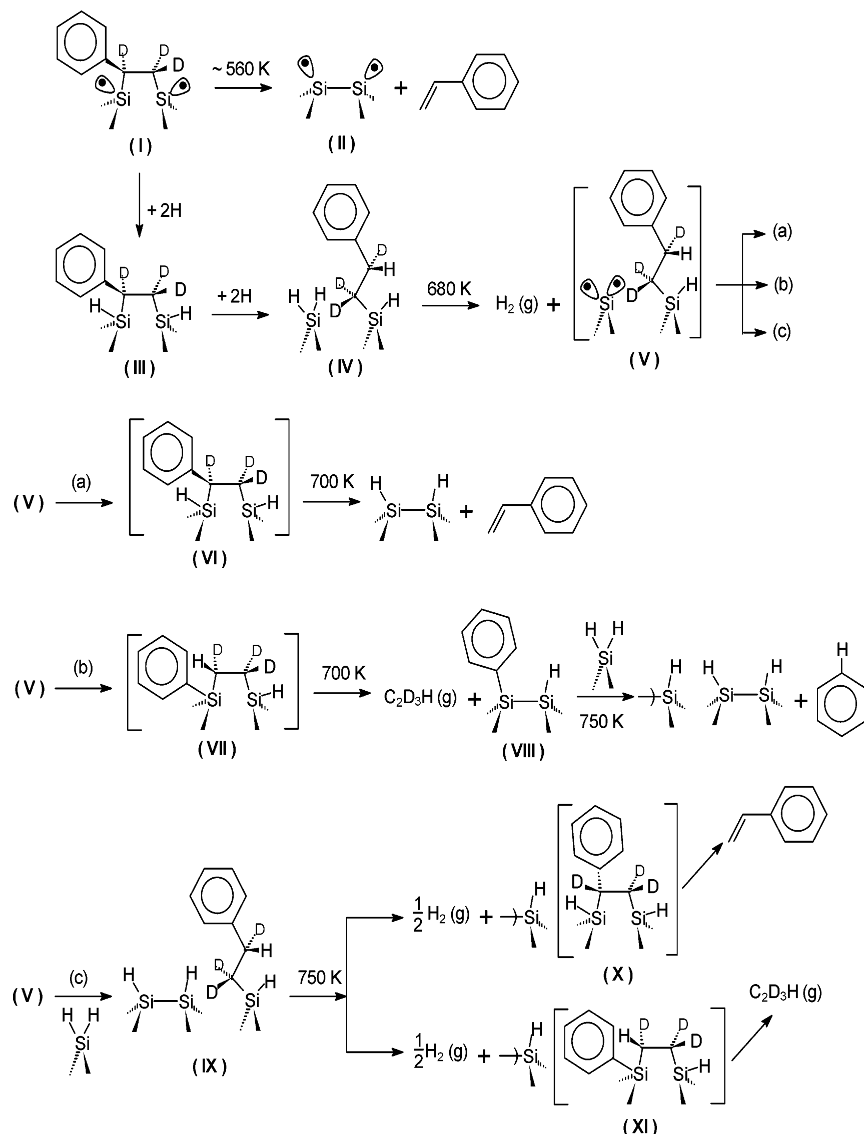

Figure 8. Proposed schemes for the adsorption, desorption, and surface reactions for styrene-d_8 on Si(100)2×1 followed by posthydrogenation.

adsorbed styrene (Figure 6). Furthermore, the "dangling" phenyl group of the adsorbed styrene appears to be not directly involved in bonding to the Si surface and also not reactive toward H atoms. The highly stable aromatic ring structure remains intact during the H postexposure and the subsequent thermal desorption process, which is also confirmed by the weaker mass 4 TDS profile for styrene-*ring*-d_5 relative to that for styrene-d_8 with H postexposure shown in Figure 7. The posthydrogenation process is therefore site-selective and occurs at the vinyl group, likely via surface-mediated enhancement.

Widdra et al.[32] reported a similar elevation in the molecular desorption temperature (from 590 to 700 K) after a high H postexposure to Si(100)2×1 exposed with ethylene. The 1,2-ethanediyl adspecies is believed to undergo hydrogenation upon high exposure of H atoms to form a surface ethyl species by breaking a Si−C σ-bond [and the (2×1) reconstruction]. Further stabilization of the ethyl−Si structure is also obtained by blocking reactive sites for both molecular desorption and decomposition pathways.[32] In the case of the styrene/Si(100)2×1 system, the adsorption is found to primarily involve a vinyl-bonded adspecies, with molecular desorption maxima found at similar temperatures for both the 2×1 and posthydrogenated sample as that for ethylene/Si(100)2×1.[32] A similar mechanism for the corresponding surface thermal chemistry could therefore be used to explain the TDS spectra in Figure 6 (and Figure 7), with the difference in the replacement of a H atom with a phenyl group on the ethylene molecule.

Figure 8 shows a proposed model for the thermal evolution of styrene-d_8 upon molecular adsorption on Si(100)2×1 at RT followed by H postexposure. Structure I illustrates the initial molecular adsorption of styrene-d_8 involving the saturation of the π bond in the vinyl group by the dangling bonds of the Si dimer and the formation of di-σ-bonded phenylethane-1,2-diyl adspecies as the [2 + 2] cycloaddition product.[37] As confirmed by the observed LEED pattern, such type of interaction does not significantly affect the (2×1) surface structure, which can be recovered upon molecular desorption near 560 K (II). Postexposure of H is believed to saturate the remaining "outside" dangling bonds of the Si dimer that are already di-σ-bonded to styrene-d_8 (III). At higher exposures, H atoms could not only attack one of the σ-bonds of the adsorbed styrene to form phenylethyl adspecies (IV) but also saturate the vacated dangling bond site, disrupting the (2×1) reconstruction and generating the observed (1×1) LEED pattern. The adsorbed H is stable up to the recombinative desorption temperature of H from silicon dihydride (~680 K). In the absence of coadsorbed hydrogen at the silicon dihydride sites, an ethyl adspecies was reported to further decompose into ethylene and hydrogen in effect by

insertion of a Si dimer atom at 600 K.[58,59] This decomposition pathway could be hindered by hydrogen occupation on the dihydride sites, which blocks the reactive neighboring sites during H postexposure, and could become available only upon annealing to 680 K. A similar mechanism could apply to the phenylethyl adspecies on Si(100), if one of the hydrogens on the adsorbed ethyl group is replaced by a phenyl group.

After the neighboring dangling bond sites have been vacated by recombinative desorption of H_2 upon annealing to 680 K, the single-σ-bonded phenylethyl adspecies (V) could undergo three possible processes upon further annealing. The phenylethyl adspecies could reoccupy the adjacent dangling bond site by an insertion reaction of a neighboring Si atom either into the C_β−H bond to form a di-σ-bonded phenylethane-1,2-diyl adspecies (VI) in process a or into C_β-phenyl bond to produce a di-σ-bonded ethane-1,2-diyl adspecies (VII) with a mono-σ-bonded phenyl adspecies in process b. Because the temperature (680 K) is already higher than the molecular desorption temperatures of styrene (560 K, Figure 6) and of ethylene (560 K),[32] once the surface hydrogen atoms begin to desorb, the as-formed di-σ-bonded phenylethane-1,2-diyl adspecies in a [2 + 2] geometry (VI) in process a and the ethane-1,2-diyl adspecies (VII) in process b would be expected to undergo immediate desorption, which accounts for the slightly higher desorption maxima of mass 112 (parent mass of styrene) and mass 31 (C_2D_3H) (not shown) at 700 K. In process b the phenyl group (VIII) recombines with a neighboring H on a dihydride site and desorbs as benzene (C_6D_5H, mass 83) at 750 K. Because the formation of benzene involves the surface reconstruction from a phase consisting of a mixture of monohydride and dihydride (i.e., a 3×1 structure with alternating dihydride and monohydride−dimer rows) to a phase with just monohydride (i.e., a 2×1 structure), the corresponding temperature of benzene formation and desorption is therefore expected to be between the H desorption temperatures for dihydride (680 K) and monohydride (800 K), which is in accord with the observed TDS maximum of mass 83 at 750 K. Finally, when the empty dangling bond sites of the single-σ-bonded phenylethyl adspecies (V) have been converted to a monohydride dimer after reacting with one of its neighboring dihydride in process c, the resulting phenylethyl adspecies (IX) could undergo similar pathways as in processes a and b. In particular, upon further annealing to 750 K in process c, the recombinative desorption of H_2 involving H atoms from a dihydride and a monohydride would induce similar Si insertion reactions in the formation of metastable di-σ-bonded phenylethane-1,2-diyl adspecies (X) and ethane-1,2-diyl adspecies (XI) that lead to desorption of styrene and ethylene, respectively. It should be noted that the difference in the H_2 recombinative desorption temperature is due to H evolution from a dihydride pair (680 K) and from a dihydride−monohydride pair (750 K). Following these three reaction pathways (a−c), the remaining hydrocarbons on the surface may undergo further decomposition into silicon carbide while the remaining H, present in the form of monohydride (on the Si dimer), could undergo recombinative desorption at 800 K. The observation of the dihydride−monohydride feature (at 750 K) is of interest because even though such a feature could exist for the H-terminated Si(100) surface, it would likely be obscured by the strong overlapping monohydride feature.

4. Conclusions

The adsorption and thermal reactions of styrene-d_8 on the 2×1 and modified Si(100) surfaces have been investigated by using TDS, AES, and LEED. At RT, the saturation coverage of styrene on Si(100)2×1 is found to be nearly identical to that of ethylene, i.e., 0.5 ML (one styrene for every surface Si dimer), and it appears to have little effect on the (2×1) LEED pattern of the Si(100) surface. Chemisorption occurs primarily by bonding through the vinyl group, with only 15% of the adsorbed styrene involving bonding through the phenyl group. Upon annealing, the adsorbate is found to undergo several plausible reactions, including molecular desorption, hydrogen abstraction, fragmentation, and/or condensation oligomerization. Similar to pyridine/Si(100)2×1,[40] the elevation of the TDS maximum for recombinative desorption involving H from the phenyl group after electron irradiation on styrene/Si(100)2×1 also suggests electron-induced oligomerization at RT.

The surface roughness of the sputtered Si surface generally provides more adsorption states and opens up new thermal dissociation pathways resulting in less molecular desorption. On the oxidized Si(100) surface, considerably reduced molecular desorption and diminished hydrogen abstraction from the vinyl group are observed, while CO production and condensation oligomerization near 1000 K are found to be plausible. Furthermore, saturation exposure of atomic H totally passivates the Si(100)2×1 surface, producing a 1×1 surface that is inert to styrene adsorption.

High postexposure of atomic hydrogen is found to stabilize the adsorption on Si(100)2×1 by transforming the di-σ vinyl-bonded cycloaddition structure of styrene (phenylethane-1,2-diyl adspecies) into a substitution adsorption structure of phenylethyl adspecies. Given the stability of the aromatic ring structure and the lack of direct bonding with the Si substrate, it is not surprising that the “dangling” phenyl group remains intact upon H postexposure at RT. Driven by thermal diffusion and desorption of hydrogen upon annealing, surface-mediated re-forming of the resulting adspecies and evolution of ethylene and benzene were observed, likely from dihydride and monohydride structures. Hydrogen therefore appears to play an important role in affecting the outcome of different chemical processes on the Si(100) surfaces.

In summary, the two functional groups (vinyl and phenyl groups) in styrene are found to exhibit different selectivity toward RT chemisorption on Si(100)2×1. In addition to different surface conditions, remarkably different surface chemical processes have been observed and could effectively be controlled on the 2×1 surface thermally and by low-energy electron irradiation and posthydrogenation.

Acknowledgment. It is our pleasure to acknowledge useful discussions with Professor Michael Chong. This work was supported by the Natural Sciences and Engineering Research Council of Canada.

References and Notes

(1) Moore, G. E. *Electronics* **1965**, *38*, 114.
(2) International Technology Road Map for Semiconductors; Semiconductor Industry Association, 2002.
(3) Bent, S. F. *Surf. Sci.* **2002**, *500*, 879−903.
(4) Tsumura, A.; Koezuka, H.; Ando, T. *Appl. Phys. Lett.* **1986**, *49*, 1210.
(5) Garito, A.; Shi, R. F.; Wu, M. *Phys. Today* **1994**, *47*, 51.
(6) Ostrick, J. R.; Dodabalapur, A.; Torsi, L.; Lovinger, A. J.; Kwock, E. W.; Miller, T. M.; Galvin, M.; Berggren, M.; Katz, H. E. *J. Appl. Phys.* **1997**, *81*, 6804.
(7) Joachim, C.; Gimzewski, J. K.; Aviram, A. *Nature* **2000**, *408*, 541.
(8) Skotheim, T. A., Elsenbaumer, R. L., Reynolds, J. R., Eds. *Handbook of Conducting Polymers*; Dekker: New York, 1998.
(9) Reddinger, J. L.; Reynolds, J. R. *Advances in Polymer Science* **1999**, *145*, 57.
(10) Hamers, R. J.; Hovis, J. S.; Greenlief, C. M.; Padowitz, D. F. *Jpn. J. Appl. Phys.* **1999**, *38*, 3879.

(11) Yates, J. T., Jr. *Science* **1998**, *279*, 335.
(12) Waltenburg, H. N.; Yates, J. T. *Chem. Rev.* **1995**, *95*, 1589.
(13) Hamers, R. J.; Wang, Y. *Chem. Rev.* **1996**, *96*, 1261.
(14) Wolkow, R. A. *Annu. Rev. Phys. Chem.* **1999**, *50*, 413.
(15) Bitzer, T.; Richardson, N. V. *Appl. Phys. Lett.* **1997**, *71*, 662.
(16) Taguchi, Y.; Fujisawa, M.; Takaoka, T.; Okada, T.; Nishijima, M. *J. Chem. Phys.* **1991**, *95*, 6870.
(17) Taguchi, Y.; Ohta, Y.; Katsumi, T.; Ichikawa, K.; Aita, O. *J. Electron Spectrosc. Relat. Phenom.* **1998**, *88*−*91*, 671.
(18) Gokhale, S.; Trischberger, P.; Menzel, D.; Widdra, W.; Droge, H.; Steinruck, H.-P.; Birkenheuer, U.; Gutdeutsch, U.; Rosch, N. *J. Chem. Phys.* **1998**, *108*, 5554.
(19) Kong, M. J.; Teplyakov, A. V.; Lyubovitsky, J. G.; Bent, S. F. *Surf. Sci.* **1998**, *411*, 286.
(20) Lopinski, G. P.; Fortier, T. M.; Moffatt, D. J.; Wolkow, R. A. *J. Vac. Sci. Technol. A* **1998**, *16*, 1037.
(21) Borovsky, B.; Krueger, M.; Ganz, E. *Phys. Rev. B* **1998**, *57*, R4269.
(22) Craig, B. I. *Surf. Sci.* **1993**, *280*, L279.
(23) Jeong, H. D.; Ryu, S.; Lee, Y. S.; Kim, S. *Surf. Sci.* **1995**, *344*, L1226.
(24) Birkenheuer, U.; Gutdeutsch, U.; Rosch, N. *Surf. Sci*. **1998**, *409*, 213.
(25) Wolkow, R. A.; Lopinski, G. P.; Moffatt, D. J. *Surf. Sci.* **1998**, *416*, L1107.
(26) Silvestrelli, P. L.; Ancilotto, F.; Toigo, F. *Phys. Rev. B* **2000**, *62*, 1596.
(27) Lu, X.; Lin, M. C.; Xu, X.; Wang, N.; Zhang, Q. *Phys. Chem. Commun.* **2001**, *13*, 1.
(28) Cheng, C. C.; Choyke, W. J.; Yates, J. T., Jr. *Surf. Sci.* **1990**, *231*, 289.
(29) Clemen, L.; Wallace, R. M.; Taylor, P. A.; Dresser, M. J.; Choyke, W. J.; Weinberg, W. H.; Yates, J. T., Jr. *Surf. Sci.* **1992**, *268*, 205.
(30) Chua, L. H.; Jackman, R. B.; Foord, J. S. *Surf. Sci.* **1994**, *315*, 69.
(31) Huang, C.; Widdra, W.; Weinberg, W. H. *Surf. Sci.* **1994**, *315*, L953.
(32) Widdra, W.; Huang, C.; Yi, S. I.; Weinberg, W. H. *J. Chem. Phys.* **1996**, *105*, 5605.
(33) Ikeda, M.; Maruoka, T.; Nagashima, N. *Surf. Sci.* **1998**, *416*, 240.
(34) Pan, W.; Zhu, T.; Yang, W. *J. Chem. Phys.* **1997**, *107*, 3981.
(35) Fisher, A. J.; Blöchl, P. E.; Briggs, G. A. D. *Surf. Sci.* **1997**, *374*, 298.
(36) Konečný, R.; Doren, D. J. *Surf. Sci.* **1998**, *417*, 169.
(37) Schwartz, M. P.; Ellison, M. D.; Coulter, S. K.; Hovis, J. S.; Hamers, R. J. *J. Am. Chem. Soc.* **2000**, *122*, 8529.
(38) Lopinski, G. P.; Wayner, D. D. M.; Wolkow, R. A. *Nature* **2000**, *406*, 48.
(39) Li, Q.; Leung, K. T. *Surf. Sci.* **2001**, *479*, 69.
(40) Li, Q.; Leung, K. T. *Surf. Sci*. **2003**, *541*, 111.
(41) Kern, W.; Puotinen, D. A. *RCA Rev.* **1970**, *31*, 187.
(42) Novak, R. E. *Solid State Technol*. **1988**, *31*, 39.
(43) NIST/EPA/NIH Mass Spectral Library; NIST'98 with Windows, version 1.7, 1996.
(44) Frisch, M. J.; Trucks, G. W.; Schlegel, H. B.; Scuseria, G. E.; Robb, M. A.; Cheeseman, J. R.; Zakrzewski, V. G.; Montgomery, J. A., Jr.; Stratmann, R. E.; Burant, J. C.; Dapprich, S.; Millam, J. M.; Daniels, A. D.; Kudin, K. N.; Strain, M. C.; Farkas, O.; Tomasi, J.; Barone, V.; Cossi, M.; Cammi, R.; Mennucci, B.; Pomelli, C.; Adamo, C.; Clifford, S.; Ochterski, J.; Petersson, G. A.; Ayala, P. Y.; Cui, Q.; Morokuma, K.; Rega, N.; Salvador, P.; Dannenberg, J. J.; Malick, D. K.; Rabuck, A. D.; Raghavachari, K.; Foresman, J. B.; Cioslowski, J.; Ortiz, J. V.; Baboul, A. G.; Stefanov, B. B.; Liu, G.; Liashenko, A.; Piskorz, P.; Komaromi, I.; Gomperts, R.; Martin, R. L.; Fox, D. J.; Keith, T.; Al-Laham, M. A.; Peng, C. Y.; Nanayakkara, A.; Challacombe, M.; Gill, P. M. W.; Johnson, B.; Chen, W.; Wong, M. W.; Andres, J. L.; Gonzalez, C.; Head-Gordon, M.; Replogle, E. S.; Pople, J. A.; Gaussian 98 (Revision A.11.3); Gaussian Inc.: Pittsburgh, PA, 2002.
(45) Foresman, J. B.; Frisch, Æ. *Exploring Chemistry with Electronic Structure Methods*, 2nd ed.; Gaussian Inc.: Pittsburgh, PA, 1996; and references therein.
(46) Suemitsu, M.; Nakazawa, H.; Miyamoto, N. *Appl. Surf. Sci.* **1994**, *82/83*, 449.
(47) Gates, S. M.; Kunz, R. R.; Greenlief, C. M. *Surf. Sci.* **1989**, *207*, 364.
(48) Taylor, P. A.; Wallace, R. M.; Cheng, C. C.; Weinberg, W. H.; Dresser, M. J.; Choyke, W. J.; Yates, J. T., Jr. *J. Am. Chem. Soc.* **1992**, *114*, 6754.
(49) Huang, C.; Widdra, W.; Wang, X. S.; Weinberg, W. H. *J. Vac. Sci. Technol. A* **1993**, *11*, 2550.
(50) Socrates, G. *Infrared Characteristic Group Frequencies*; Wiley: New York, 1980.
(51) Li, Q., Ph.D. Thesis, University of Waterloo, Waterloo, Ontario, Canada, 2004.
(52) Ageev, V. N. *Prog. Surf. Sci.* **1994**, *47*, 55 and references therein.
(53) Young, R. Y.; Brown, K. A.; Ho, W. *Surf. Sci.* **1995**, *336*, 85.
(54) Imamura, Y.; Matsui, N.; Morikawa, Y.; Hada, M.; Kubo, T.; Nishijima, M.; Nakatsuji, H. *Chem. Phys. Lett.* **1998**, *287*, 131.
(55) Hu, D. Q.; MacPherson, C. D.; Leung, K. T. *Surf. Sci.* **1992**, *273*, 21.
(56) MacPherson, C. D.; Hu, D. Q.; Doan, M.; Leung, K. T. *Surf. Sci.* **1992**, *310*, 231.
(57) MacPherson, C. D.; Hu, D. Q.; Leung, K. T. *Surf. Sci.* **1995**, *322*, 58.
(58) Keeling, L. A.; Chen, L.; Greenlief, C. M. *Chem. Phys. Lett.* **1994**, *217*, 136.
(59) Schmidt, J.; Stuhlmann, C.; Ibach, H. *Surf. Sci.* **1994**, *302*, 10.